

Novel organosoluble filiform zirconium phosphonates with a layered mesoporous backbone†

Xuebing Ma,* Jing Liu, Linshan Xiao, Rui Chen, Jinqin Zhou and Xiangkai Fu

Received 24th September 2008, Accepted 14th November 2008

First published as an Advance Article on the web 5th January 2009

DOI: 10.1039/b816542d

A novel type of organosoluble and filiform zirconium phosphonate with a layered mesoporous backbone functionalized with hydroxyl and amino groups was prepared by the reaction of a functionalized phosphoric acid with $\text{ZrOCl}_2 \cdot 8\text{H}_2\text{O}$. These filiform zirconium phosphonates has good solubility ($0.21\text{--}0.71\text{ g mL}^{-1}$) in certain organic solvents (such as toluene, chloroform, tetrahydrofuran and ethyl acetate), are immiscible in some other solvents (hexane, cyclohexane, petroleum ether and ethanol), and can be recovered from organic solvents in high yield (95–100%) by precipitation.

Introduction

The immobilisation of homogeneous catalysts is usually used to facilitate the separation of relatively expensive catalysts from reaction mixtures.¹ A successful homogeneous catalyst immobilized on insoluble inorganic solid supports such as silica gel or zeolites can positively influence the catalytic performance; for example, the catalytic activity, chemoselectivity and enantioselectivity can increase due to the site isolation effect,² the confinement effect,³ and the cooperative effect of the support backbone.⁴ Unfortunately, due to the problem of mass transfer, most examples of catalysts supported on inorganic materials have tended to have inferior catalytic properties compared to their homogeneous counterparts. Therefore, a new strategy, using soluble polymers and dendrimers as supports in catalysis,⁵ has recently been highlighted as a new option for the immobilization of homogeneous catalysts. However, owing to the flexibility of soluble polymers and dendrimers with linear and cross-linked structures, these catalysts can become entangled or twisted, shielding their active catalytic centers and lowering their catalytic properties.

Due to applications in the field of catalysis,⁶ adsorption, ion exchange and/or functional materials,⁷ layered and porous

zirconium phosphonates have continued to be of considerable interest in recent years, but unfortunately they are immiscible in organic solvents. In this paper, by the choice of organic pendant groups bonded to the backbone of a layered and porous zirconium phosphate, we have developed the first example of an organosoluble and filiform zirconium phosphonate (Fig. 1). This catalyst is soluble in toluene, chloroform, tetrahydrofuran and ethyl acetate, and immiscible in hexane, cyclohexane, petroleum ether and ethanol. As an ideal scaffold for the immobilization of expensive metals such as Pt, Rh and Pd, these novel zirconium phosphonates **1–4** functionalized by amino and hydroxyl complex groups will fill a gap in the field of homogeneous catalysis, and combine the individual advantages of the organosolubility of organic polymers and the rigid and porous properties of inorganic solids. Furthermore, the zirconium phosphonates **1–4** are readily recyclable by precipitation.⁸

Experimental

General

Infrared spectra were recorded on a Spectrum GX using polystyrene as a standard (KBr pellet). TG analysis was performed on a SBTQ600 Thermal Analyzer (USA) with a heating rate of

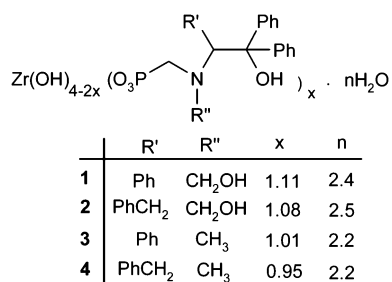


Fig. 1 The structures of the organosoluble filiform zirconium phosphonates **1–4**.

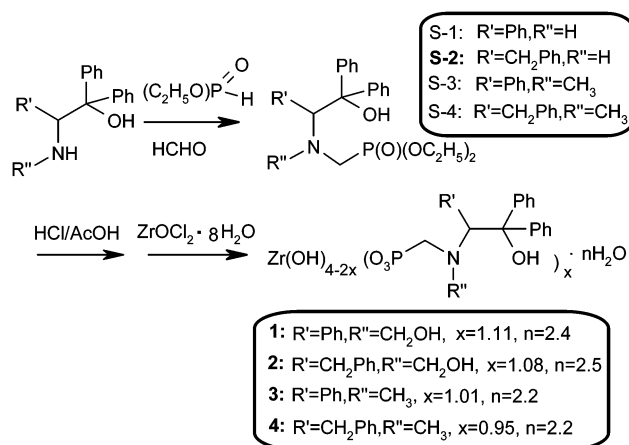


Fig. 2 The synthesis of zirconium phosphonates **1–4**.

College of Chemistry and Chemical Engineering, Southwest University, Chongqing, 400715, P. R. China. E-mail: zcjl23@swu.edu.cn; Fax: +86 23 68253237; Tel: +86 23 6825 4963

† Electronic supplementary information (ESI) available: NMR and IR spectra, and TEM images. See DOI: 10.1039/b816542d

20 °C min⁻¹ from room temperature to 1000 °C under flowing compressed N₂ (100 mL min⁻¹). ¹H, ¹³C and ³¹P NMR were performed on a Bruker AV-300 NMR instrument at ambient temperature at 300, 75 and 121 MHz, respectively. All of the chemical shifts were reported downfield in ppm relative to the hydrogen, carbon and phosphorus resonance of TMS, chloroform-*d*₁ and H₃PO₄ (85%) respectively. The interlayer spacings were obtained on a DX-1000 automated X-ray power diffractometer, using Cu K α radiation and internal silicon powder standard with all samples. The patterns were generally measured between 2.00° and 35.00° (2 θ) with a step size of 1° min⁻¹ and X-ray tube settings of 40 kV and 2.5 mA. C, H and N elemental analysis was obtained from an EATM 1112 automatic elemental analyzer instrument (Thermo, USA). The size and morphology of as-synthesized samples were determined by a Hitachi model H-800 transmission electron microscope. N₂ adsorption-desorption analysis was carried out at 77 K on an Autosorb-1 apparatus (Quantachrome). The surface areas of zirconium phosphonates were determined by using the BET equation, and the pore diameters were estimated according to the BJH model.

All materials and reagents used were of analytical grade (Astara) and were used as supplied without further purification. The zirconium phosphonates 1–4 were prepared following the synthetic route described in Fig. 2.

Synthesis of phosphonates S-1–4

To a mixture of 2 mL of THF, 4 mL of H₂SO₄ (25%) and formaldehyde (2.0 g, 24.7 mmol, 37%) was added dropwise 40 mL of THF solution containing β -aminoalcohol or *N*-methyl- β -aminoalcohol (10 mmol) over 30 min. This was stirred for 1 h at 40 °C, and concentrated under the reduced pressure. The residue was charged with diethyl phosphite (1.66 g, 12 mmol) and cationic exchange resin (0.5 g). The reaction mixture was stirred at 60 °C for 6 h, and the cationic exchange resin was removed by filtration. For the phosphonates starting from β -aminoalcohol (R'' = H), the reaction mixture was evaporated under reduced pressure and 10 mL of ethyl acetate was added. White needles of the phosphonates S-1 (3.7 g, 82%) and S-2 (3.4 g, 76%) were obtained by filtration and drying at 60 °C under reduced pressure. Otherwise, for the phosphonates starting from *N*-methyl- β -aminoalcohol (R'' = CH₃), the reaction mixture was evaporated under the reduced pressure to give a yellow oily liquid. The white phosphonates S-3 (3.5 g, 78%) and S-4 (3.7 g, 79%) were purified by silica gel column chromatography using ethyl acetate/petroleum ether (60–90 °C) (v/v = 1:10), evaporation and drying under reduced pressure at 60 °C for 10 h.

Phosphonate S-1. Mp 136–137 °C (recrystallized from ethyl acetate). δ_{H} (300 MHz, CDCl₃, Me₄Si) 7.63 (2 H, d, Ph, ³J_{1,3} = 7.56 Hz), 7.35 (2 H, d, Ph, ³J_{1,3} = 7.7 Hz), 7.25 (1 H, d, Ph, ³J_{1,3} = 7.26 Hz), 7.11–7.06 (3 H, m, Ph), 7.02–6.99 (7 H, Ph, m), 5.37 (1 H, s, OCH₂), 4.52 (1 H, s, OCH₂), 4.38 (1 H, s, CH), 4.08–3.93 (4 H, m, OCH₂), 2.93–2.55 (2 H, m, CH₂P, AB system), 1.31–1.04 (6 H, m, CH₃). δ_{C} (300 MHz, CDCl₃) 145.1, 142.4, 136.8, 130.0, 128.2, 127.8, 127.5, 127.3, 127.0, 126.7, 126.6 (Ph), 89.6 (C–OH, s), 85.9 (CH₂OH, s), 77.5 (NCH, s), 62.3 (OCH₂, d, ²J_{cp} = 46.6 Hz), 46.0 (CH₂P, d, ¹J_{cp} = 165.2 Hz), 16.4 (CH₃, t, ³J_{cp} = 6.4 Hz). δ_{P} (300 MHz, CDCl₃, 85% H₃PO₄) 24.8–24.6 (m). IR (KBr):

ν_{max} /cm⁻¹ 3417w (O–H), 3063, 3032s (Ph–H), 2983–2728s (CH₃, CH₂, CH), 1601s, 1545s, 1492s (Ph), 1446w, 1387s (CH₃, CH₂, CH), 1031vs (PO₃). Found: C, 71.19; H, 7.40; N, 3.16. Anal. Calcd for C₂₆H₃₂NO₅: C, 71.20; H, 7.37; N, 3.19%.

Phosphonate S-2. Mp 141–142 °C (recrystallized from ethyl acetate). δ_{H} (300 MHz, CDCl₃, Me₄Si) 7.69 (2 H, d, Ph, ³J_{1,3} = 7.23 Hz), 7.57–7.10 (13 H, m, Ph), 5.09 (1 H, s, OCH₂), 4.43 (1 H, s, OCH₂), 4.15 (1 H, t, CH), 3.89–3.76 (4 H, m, OCH₂), 2.72–2.56 (2 H, m, CH₂P, AB system), 2.46–2.38 (2 H, m, CH₂), 1.24–1.12 (3 H, m, CH₃). δ_{C} (300 MHz, CDCl₃) 145.2, 142.6, 139.6, 129.2, 128.4, 128.1, 127.8, 127.3, 126.8, 126.7, 126.2, 125.9 (Ph), 88.2 (COH), 85.7 (CH₂OH), 73.9 (NCH, d, ³J_{cp} = 15.5 Hz), 62.2 (OCH₂, d, ³J_{cp} = 43.2 Hz), 50.8 (CH₂P, d, ¹J_{cp} = 165.6 Hz), 38.3 (CH₂), 16.3 (CH₃, t, ³J_{cp} = 6.2 Hz). δ_{P} (300 MHz, CDCl₃, 85% H₃PO₄) 24.4 (t). IR (KBr): ν_{max} /cm⁻¹ 3483s (O–H), 3331vs, 3285vs, 3244vs, 3170vs (Ph), 2940s, 2886s (CH₃, CH₂, CH), 1631s, 1599s (Ph), 1450w, 1383vs (CH₃, CH₂, CH), 1025vs (PO₃). Found: C, 71.63; H, 7.63; N, 3.08. Anal. Calcd for C₂₇H₃₄NO₅: C, 71.65; H, 7.59; N, 3.10%.

Phosphonate S-3. Mp 138–139 °C. δ_{H} (300 MHz, CDCl₃, Me₄Si) 7.66 (2 H, d, Ph, ³J_{1,3} = 6.0 Hz), 7.39–7.21 (3 H, m, Ph), 7.13–7.04 (10 H, m, Ph), 7.18–7.01 (Ph, 10 H, m), 5.39 (1 H, s, NCH), 4.49 (2 H, d, PCH₂N, ²J_{HP} = 48.0 Hz), 4.13–3.96 (4 H, m, OCH₂), 2.96–2.60 (3 H, m, NCH₃), 1.30–1.19 (6 H, m, CH₃). δ_{C} (75 MHz, CDCl₃) 146.5, 145.5, 144.9, 129.8, 127.9, 127.6, 127.4, 127.1, 126.8, 125.9, 125.6, 125.5 (Ph), 85.7 (C–O), 73.7 (CHN), 63.3 (OCH₂, d, ²J_{cp} = 6.0 Hz), 61.7 (NCH₃, d, ³J_{cp} = 6.0 Hz), 46.6 (PCH₂, d, ¹J_{cp} = 100.5 Hz). δ_{P} (121 MHz, CDCl₃, 85% H₃PO₄) 18.3 (s). IR (KBr): ν_{max} /cm⁻¹ 3286s (O–H), 3084w, 3055w, 3025s (Ph), 2964w, 2936 w, 2884w, 2796w (CH₃, CH₂, CH), 1601s, 1492s (Ph), 1060 vs (PO₃). Found: C, 73.84; H, 7.72; N, 3.24. Anal. Calcd for C₂₆H₃₂NO₄: C, 73.90; H, 7.65; N, 3.32%.

Phosphonate S-4. Mp 144–145 °C. δ_{H} (300 MHz, CDCl₃, Me₄Si) 7.66–7.57 (4 H, dd, Ph), 7.34–7.08 (11 H, m, Ph), 6.19 (–OH, s), 4.16–3.97 (2 H, m, OCH₂), 3.71 (1 H, t, NCH, ³J_{1,3} = 18.6 Hz), 3.37–3.26 (2 H, m, OCH₂), 2.97, 2.65–2.47 (2 H, dd, PhCH₂), 2.21 (3 H, s, NCH₃), 1.26 (3 H, t, CH₂CH₃, ³J_{1,3} = 7.0 Hz), 0.96 (3 H, t, CH₂CH₃, ³J_{1,3} = 7.0 Hz). δ_{C} (75 MHz, CDCl₃) 147.7, 145.0, 140.4, 129.7, 128.3, 128.0, 128.0, 126.8, 125.9, 125.8, 125.2, 125.2 (Ph), 81.5 (COH), 72.3 (CHN, d, ³J_{cp} = 9.0 Hz), 62.2 (OCH₂, d, ²J_{cp} = 137.3 Hz), 48.31 (PCH₂, d, ¹J_{cp} = 171.8 Hz), 47.4 (NCH₃), 31.8 (CH₂), 16.3 (CH₃, t, ³J_{cp} = 5.1 Hz). δ_{P} (121 MHz, CDCl₃, 85% H₃PO₄) 28.5. IR (KBr): ν_{max} /cm⁻¹ 3420vs (O–H), 3171s, 3119vs (Ph) 2982w, 2947w, 2892s (CH₃, CH₂, CH), 1641vs (Ph), 1117s (PO₃). Found: C, 74.21; H, 7.92; N, 3.20. Anal. Calcd for C₂₇H₃₄NO₄: C, 74.28; H, 7.87; N, 3.21%.

Preparation of zirconium phosphonates (1–4)

A mixture of the phosphonate S-1 (4.4 g, 10 mmol), 50 mL of acetic acid and 10 mL of hydrochloric acid (36%) was stirred at 80 °C for 8 h. Zirconium oxychloride (3.4 g, 10 mmol) in 10 mL of deionized water was added dropwise and stirred continued at 80 °C for 4 h. The white solid zirconium phosphonate 1 was filtered, washed with sodium carbonate (0.1 mol L⁻¹) and water to achieve pH = 6–7, and then washed with ethanol (30 mL \times 3)

and dried at 60 °C for 24 h under reduced pressure. White zirconium phosphonates **2–4** were prepared according to the same procedure.

Zirconium phosphonate 1. 7.6 g in 90% yield. δ_P (121 MHz, CDCl_3 , 85% H_3PO_4) 12.3 (s, bound). IR (KBr): $\nu_{\text{max}}/\text{cm}^{-1}$ 3407s (OH), 3060s, 3028s (Ph), 2820w, 2756w (CH_3 , CH_2 , CH), 1681s, 1596s, 1493s (Ph), 1448s, 1358w (CH_3 , CH_2 , CH), 1029vs (PO_3Zr). Found: C, 47.20; H, 4.48%; N, 2.14. Anal. Calcd for $\text{C}_{24.42}\text{H}_{31.0}\text{N}_{1.11}\text{O}_{9.73}\text{P}_{1.11}\text{Zr}$: C, 47.22; H, 4.94; N, 2.50%.

Zirconium phosphonate 2. 7.9 g in 92% yield. δ_P (121 MHz, CDCl_3 , 85% H_3PO_4) 12.9 (s, bound). IR (KBr): $\nu_{\text{max}}/\text{cm}^{-1}$ 3409s (–OH), 3299s (Ph), 2956s, 2887s (CH_3 , CH_2 , CH), 1631s, 1587s (Ph), 1382vs (CH_3 , CH_2 , CH), 1029s (PO_3Zr). Found: C, 47.36; H, 4.78; N, 2.30. Anal. Calcd for $\text{C}_{24.84}\text{H}_{32.76}\text{N}_{1.08}\text{O}_{9.74}\text{P}_{1.08}\text{Zr}$: C, 47.54; H, 5.27; N, 2.41%.

Zirconium phosphonate 3. 7.2 g in 88% yield. δ_P (121 MHz, CDCl_3 , 85% H_3PO_4) 13.44 (s, bound). IR (KBr): $\nu_{\text{max}}/\text{cm}^{-1}$ 3408s (OH), 3060s, 3026s (Ph), 2820w, 2797w (CH_3 , CH_2 , CH), 1681s, 1597s, 1493s (Ph), 999vs (PO_3Zr). Found: C, 47.26; H, 4.67; N, 2.23. Anal. Calcd for $\text{C}_{22.22}\text{H}_{28.60}\text{N}_{1.01}\text{O}_{8.22}\text{P}_{1.01}\text{Zr}$: C, 47.33; H, 5.12; N, 2.51%.

Zirconium phosphonate 4. 7.3 g in 88% yield. δ_P (121 MHz, CDCl_3 , 85% H_3PO_4) 11.57 (s, bound). IR (KBr): $\nu_{\text{max}}/\text{cm}^{-1}$ 3408s (OH), 3060s, 3028s (Ph), 2828w, 2795w (CH_3 , CH_2 , CH), 1681s, 1597s, 1493s (Ph), 997vs (PO_3Zr). Found: C, 47.31; H, 4.46; N, 2.22. Anal. Calcd for $\text{C}_{21.85}\text{H}_{29.30}\text{N}_{0.95}\text{O}_{8.10}\text{P}_{0.95}\text{Zr}$: C, 47.24; H, 5.02; N, 2.40%.

Results and discussion

Chemical and physical characterization

Chemical analysis. In a sealed plastic container, a mixture of 2 mL of deionized water and 50 mg of zirconium phosphonate **1–4** was treated with 2 mL of hydrofluoric acid (30%) and stirred at room temperature for 6 h. Due to the formation of the complex ZrF_6^{2-} , **1–4** decomposed. In the resulting solution, the zirconium(IV) and phosphonic acid content was determined by colorimetry and ^{31}P NMR respectively. The molar ratio of the appended organic moieties to zirconium(IV) in **1–4** were 1.11, 1.08, 1.01 and 0.95 respectively. The empirical formulae of **1–4** were ascertained by elemental analysis and TG analysis, and are shown in Fig. 1.

Infrared spectroscopy. In order to ascertain the attachment of the functional organic moieties on the backbone of zirconium phosphonate, infrared spectra of **1–4** were recorded in the range 4000–400 cm^{-1} . The strong and wide absorption band extending from 3700 to 2500 cm^{-1} and centered at 3407 cm^{-1} was assigned to the –O–H stretching vibration, which verified the presence of a hydrogen bond between the hydroxyl groups on the internal and external surfaces of the zirconium layers. The sharp absorption bands at 1680–1450 cm^{-1} and 700–670 cm^{-1} were respectively attributed to the characteristic absorptions and the flexing vibration of the phenyl group. The absorption bands at

about 1030 cm^{-1} were caused by the Zr–O–P stretching vibration. From this data, it was concluded that functional organic moieties containing a β -aminoalcohol were anchored on the frame of zirconium phosphonate, whose solution ^{31}P NMR had a resonance in the range –10 to +20 ppm.

Thermal gravimetric analysis. From the TG curves shown in Fig. 3, it can be deduced that **1–4** lost 2.2–2.5 molar equivalents of surface-bound or intercalated water below 200 °C, and the process, as usual, was endothermic. The sharp weight loss in the temperature range of 200–500 °C, accompanied by endothermic peaks in the DSC curves, corresponded to the decomposition of the appended organic fragments. After the volatilization of organic fragments, zirconium phosphonates **1–4** were converted to zirconium phosphate. In the same temperature range, the losses of pendant organic moieties by TG analysis were 62.77, 61.75, 61.99 and 61.24 wt% respectively, which were 1.8–3.4% wt% higher than that of the theoretical values; this can probably be attributed to the simultaneous dehydration of the internal and external free hydroxyl groups. Finally, the small weight losses between 800 or 900 °C and 1200 °C were due to phase changes from layered to cubic ZrP_2O_7 , as confirmed by XRD.⁹

Powder XRD. The interlayer distances or d -spacings of zirconium planes for crystalline zirconium phosphonates can be determined from the $00n$ peaks in the powder XRD pattern (via the Bragg equation, $n\lambda = 2d\sin\theta$). The d -spacings for **1–4** are given in Fig. 4. As can be seen from Fig. 4, except for zirconium phosphonate **3**, the other XRD patterns displayed a broad 001 peak (the lowest-angle diffraction peak in the pattern), without higher-order $00n$ peaks at larger angles and lower intensities.

Assuming a perpendicular orientation of the organic chains and the bimolecular layers of β -aminoalcohol moieties with an “end-to-end” structure between neighbouring zirconium planes, the predicted d -spacings of the zirconium phosphonates are obtained by summing the zirconium phosphate layer thickness (3.2 Å),¹⁰ twice the normal distance (projection along the P–C bond axis) from the phosphorus atom to the farthest hydrogen atom in the organic functional group, and twice the hydrogen atomic radius (0.35 Å).¹¹ Therefore, the calculated interlayer spacings of **1–4** by the MM2 method are 22.1, 21.1, 19.9 and 18.9 Å respectively. The calculated interlayer spacings of zirconium phosphonates **1–3** are in good agreement with the experimental values, with a just a small deviation (below 0.6 Å). This small deviation is most likely due to the two assumptions inherent in this simple model: (i) that the organic groups are perpendicular to the plane containing the zirconium atoms; and (ii) that the contact between the organic groups in adjacent layers is “end-to-end”. As an example, the idealized chain geometry of zirconium phosphonates **1** is shown in Fig. 5. In the idealized model, the hydroxyl groups in the organic moieties form hydrogen bonds with each other (verified by the strong broad infrared absorption band), making the zirconium atoms self-assemble in the same plane.

However, for zirconium phosphonate **4** there was a large deviation between the actual interlayer spacing of 14.18 Å and the predicted interlayer spacing of 18.9 Å by MM2 based on the assumption of an “end-to-end” structure. This is probably because the surface hydroxyl groups on the zirconium plane

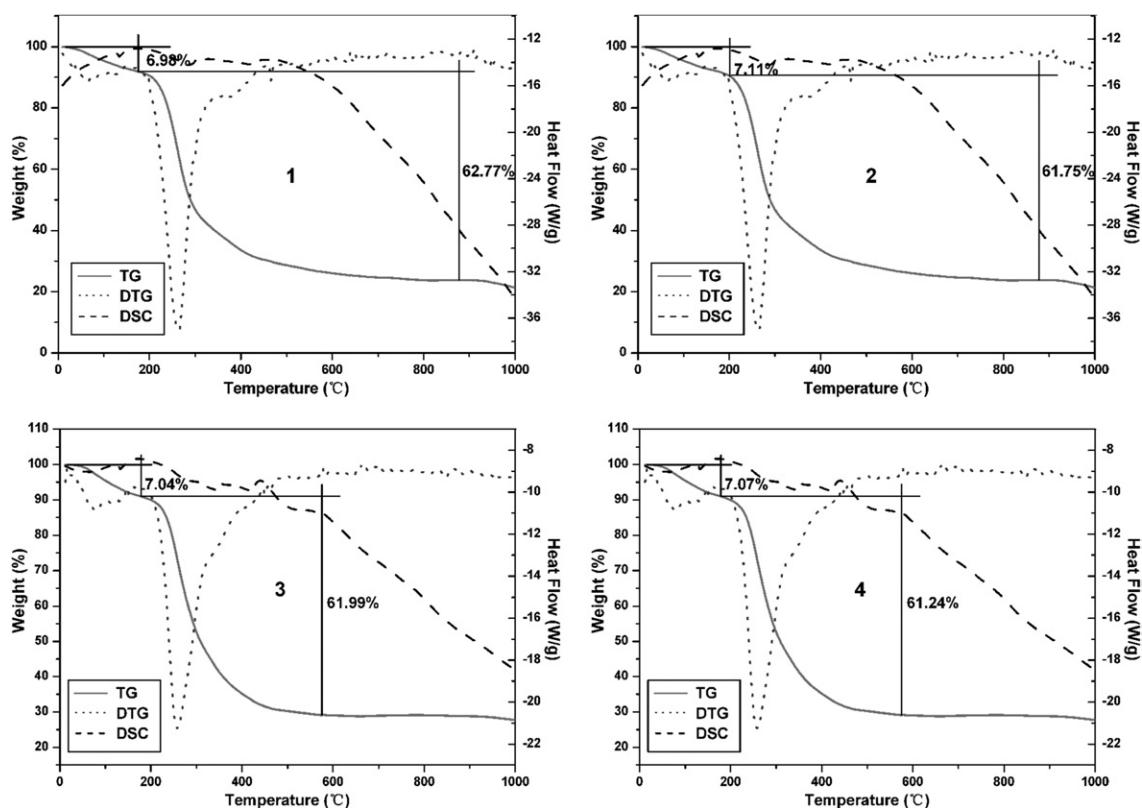


Fig. 3 The TG curves of the zirconium phosphonates 1–4.

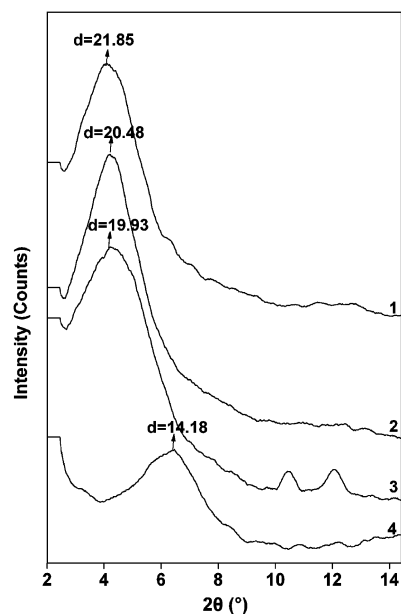


Fig. 4 X-Ray diffraction patterns displaying the $00n$ peaks of zirconium phosphonates 1–4.

increased in number with the decrease of x values from 1.11 to 0.95, providing enough large spaces to satisfy the different structural possibilities for the arrangement of organic moieties between the neighbouring zirconium planes. Moreover, in regards to the first assumption mentioned above, experimental

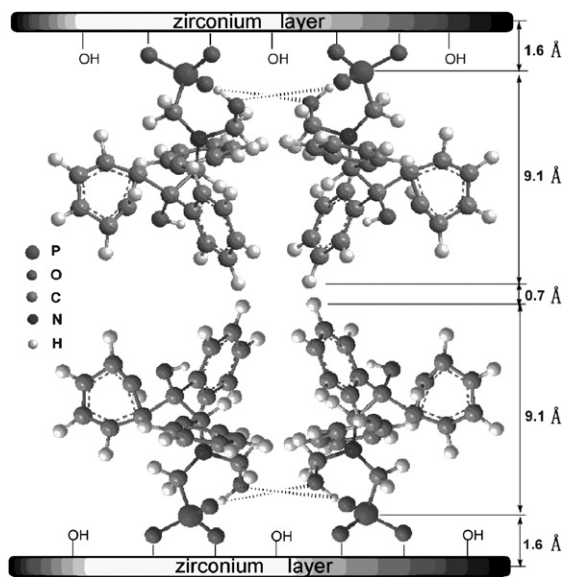


Fig. 5 The idealized structure of zirconium phosphonate 1.

observations from the Rietveld refinement of the structure of zirconium bis(phenylphosphonate) and zirconium *p*-aminobenzylphosphonates both show that the P–C bond is not normal to the layer and is in fact tilted by approximately 30° .¹² In the light of the possibility of forming hydrogen bonds between the hydroxyl groups, the idealized structure of **4** was refined by the MM2 method (see Fig. 6), although the actual structure most

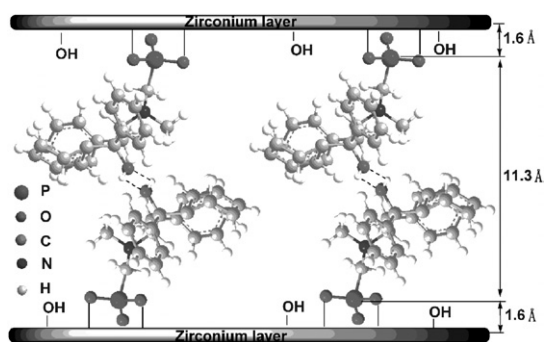


Fig. 6 The idealized structure of zirconium phosphonate 4.

likely includes other conformations not depicted in Fig. 5 and Fig. 6. The calculated interlayer spacing of the refined model shown in Fig. 6 is 14.5 Å, slightly higher than the detected value (14.18 Å), with a small deviation (0.32 Å).

Nitrogen adsorption–desorption isotherms. Following the BET treatment of the isotherms, low specific surface areas were found

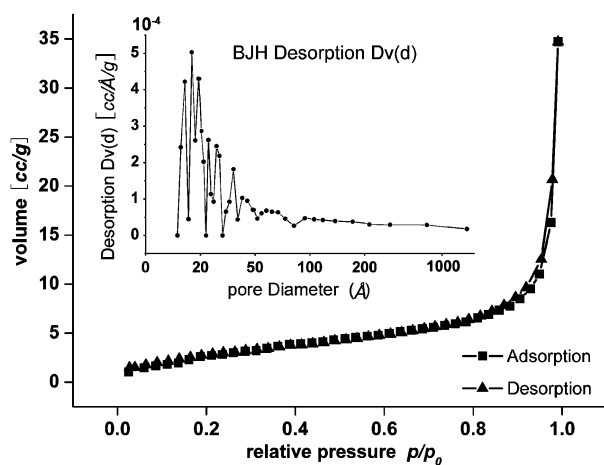


Fig. 7 The nitrogen adsorption–desorption isotherm and pore distribution of zirconium phosphonate 2.

Table 1 The physical properties of zirconium phosphonates 1–4

Phosphonate	Elemental analysis		Organic moieties (%) ^a		Surface area (m ² /g)	Pore volume (× 10 ⁻² cm ³ /g)	Average pore diameter (nm)
	Calc.	Found	Calc.	Found			
1	C	47.22	47.20	59.4	12.3	9.31	3.02
	H	4.94	4.48	62.8			
	N	2.50	2.14				
2	C	47.54	47.36	59.6	11.0	5.34	1.94
	H	5.27	4.78	61.8			
	N	2.41	2.30				
3	C	47.33	47.26	59.1	10.7	6.63	2.47
	H	5.12	4.67	62.0			
	N	2.51	2.23				
4	C	47.24	47.31	59.4	9.4	4.45	1.90
	H	5.02	4.46	61.2			
	N	2.40	2.22				

^a From thermogravimetric analysis.

for solid-state 1–4 were found (9.4–12.3 m² g⁻¹). The nitrogen adsorption–desorption isotherm of zirconium phosphonate 2 (Fig. 7) was type IV, with a sharp increase in N₂ adsorption at higher P/P₀ values (~0.9) and a distinct hysteresis loop (type H1), with an almost parallel adsorption and desorption.

For zirconium phosphonates 1, 3 and 4, a distinct hysteresis loop (type H3) without parallel or overlapped nitrogen adsorption–desorption isotherms was observed. Based on the desorption isotherm, BJH analysis gave a broad and non-uniform distribution of pore size (in the range 1.5–5 nm) for 1–4. The physical properties of 1–4 are listed in Table 1.

Surface morphology. Generally, zirconium phosphonates are spheroid or featureless and submicron in size with a layered crystalline structure.^{13,6d-f} The as-synthesized samples of the layered mesoporous zirconium phosphonates 1–4 were dispersed in cyclohexane, stirred for 2 h and their morphology determined by transmission electron microscopy. Surprisingly, we saw a novel type of filiform structure (Fig. 8).

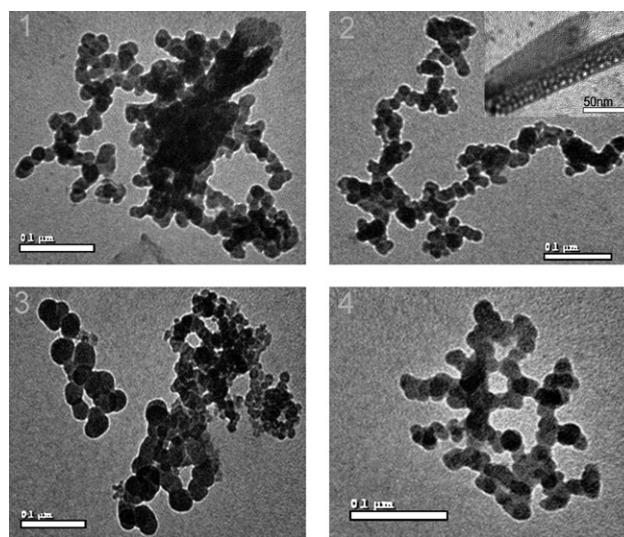


Fig. 8 TEM images of the layered mesoporous zirconium phosphonates 1–4.

From the TEM images, it can be seen that the filiform structures were produced with widths of 20–30 nm and lengths up to hundreds of micrometers. Furthermore, according to the XRPD analysis, the zirconium phosphonates **1–4** were layered mesoporous materials with an interlayer spacing of about 2 nm (except for zirconium phosphonate **4**); see Fig. 4, 5 and 6. As an example, based on the interlayer spacings of zirconium phosphonates **1–3** (19.9–21.9 nm) determined by XRPD, it can be deduced that each filiform structure consists of stacks of 10–15 layers of zirconium phosphonates, resulting in few mesopores with the average dimensions of 1.9–3.2 nm (see inset of Fig. 8-2).

Solubility in organic solvents

Relation between the organosolubility and the substituted group in zirconium phosphonates. Reported zirconium phosphonates have seldom been soluble in organic solvents; there is just one report of an organosoluble zirconium phosphonate, with composition $[(iPrO)_3Zr(\mu-OiPr)_2(\mu-OPOPh_2)Zr(OiPr_2)PPh_2(O)(OH)]$, which was prepared in high yield by the reaction of $Ph_2P(O)(OH)$ with zirconium isopropoxide at $-60^\circ C$ in toluene.¹⁴ However, due to the lack of complexing groups for catalytic transition metals, this type of organosoluble zirconium phosphonate has not received much attention in the field of catalysis. It is therefore noteworthy that the zirconium phosphonates **1–4** synthesised in this work show good solubility ($0.3\text{--}0.7\text{ g mL}^{-1}$) in various organic solvents (Table 2).

From Table 2, it can be seen that **1** is readily soluble in $CHCl_3$ and THF, with a solubility of about 0.57 and 0.59 g mL^{-1} respectively. Zirconium phosphate **2** (where R' is $PhCH_2$ instead of Ph) can be dissolved in other solvents such as toluene, benzene and ethyl acetate ($0.21\text{--}0.71\text{ g mL}^{-1}$), whereas **3** and **4** (where R'' is a methyl group instead of a hydroxymethyl group) are only soluble in THF and toluene. All four zirconium phosphonates are insoluble in ethanol, hexane, petroleum ether and cyclohexane. It is therefore clear that the solubility properties of **1–4** are related to the identity of the substituted groups (R' and R'').

To further illustrate the relationship between the organosolubility and the number of phenyl groups attached to the backbone of the zirconium phosphonates, one of the phenyl groups at the hydroxyl group position in **1** was changed to be a hydrogen atom instead of a phenyl group. This zirconium phosphonate was immiscible in organic solvents,^{6d} although the corresponding titanium phosphonate was (slightly) soluble only in ethanol ($30\text{--}50\text{ mg mL}^{-1}$).¹⁵ Zirconium phosphonates with more phenyl groups and without amino or hydroxyl groups, $Zr(OH)_{1.8}[O_3P(CH_2)_nPPh_2]_{1.1}$ ($n = 2\text{--}6$) and $Zr(OH)_{2.2}[O_3P(CH_2)_nN(CH_2CH_2PPh_2)_2]_{0.9}$ ($n = 2\text{--}6$), were

Table 2 The organosolubilities of zirconium phosphonates **1–4** in organic solvents (g mL^{-1})^a

Phosphonate	Chloroform	THF	Toluene	Benzene	Ethyl acetate
1	0.57	0.59	0	0	0
2	0.46	0.65	0.71	0.21	0.51
3	0	0.47	0.57	0	0
4	0	0.52	0.53	0	0

^a Determined in 1 mL of solvent at $25^\circ C$.

also synthesized by the reaction of functionalized phosphoric acids with $ZrOCl_2 \cdot 8H_2O$, but they were completely insoluble in organic solvents. Therefore, we can conclude that the number of phenyl, amino and hydroxyl groups in the pendant organic moieties and their cooperative effect plays an important role in the solubility of zirconium phosphonates **1–4** in organic solvents.

Relation between organosolubility and filiform structure. The solubility of **1–4** in various organic solvents is related to the filiform structure as well as the pendant organic moieties. If during the preparation stirring was continued for over 12 h at $70\text{--}80^\circ C$, the zirconium phosphonates **1–4** became insoluble in the organic solvents mentioned above, despite having the same chemical composition. TEM of the modified zirconium phosphonates **1–4** showed that surprisingly the filiform morphology of zirconium phosphonates **1–4** had been converted to the typical amorphous (mesoporous) and crystalline (layered) nanoparticles, with the same interlayer spacings (Fig. 9) as the reported insoluble zirconium phosphonates. The conversion of the filiform structure to the amorphous and crystalline states may therefore be the reason for the organosoluble zirconium phosphonates **1–4** becoming insoluble in organic solvents at stirring times above 12 h.

Recycling from organic solvents

We considered that the different solubilities of zirconium phosphonates **1–4** in organic solvents could be beneficial in achieving homogeneous catalysis in various solvents and recycling by

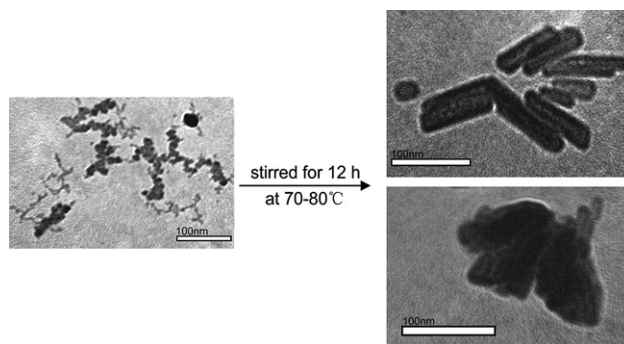


Fig. 9 The conversion of the filiform structure of zirconium phosphonates to the mesoporous and layered states.

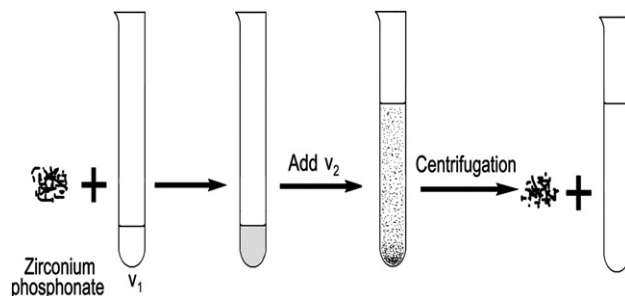


Fig. 10 The recycling procedure of zirconium phosphonates **1–4**.

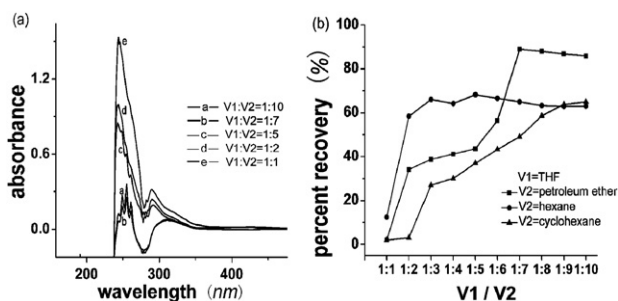


Fig. 11 (a) UV adsorption in solution and (b) percent recovery of zirconium phosphonate **2** with different volume ratios of good solvent to poor solvent (v_1/v_2).

means of precipitation. To assess the ease of recycling on a small scale, the filiform zirconium phosphonates **1–4** were dissolved in one of the good solvents (v_1), which are generally suitable for homogeneous catalytic reactions. Upon adding a poor solvent (v_2), zirconium phosphonates **1–4** precipitated out, providing a means of separation (Fig. 10).

For example, 0.6 mg of phosphonate **2** was dissolved in 1 mL of the first solvent (v_1), and the second solvent (v_2) was then added in a volume ratio (v_2/v_1) between 10:1 and 1:1. The phosphonate **2** precipitated as a solid and was separated from the mixture centrifugally. From the concentration of zirconium phosphonate in the organic phase as determined by UV spectroscopy, the percent recovery (2–89%) could be calculated (Fig. 11). From Fig. 11, it can be seen that THF as the first solvent (v_1) and petroleum ether as the second solvent (v_2) is the optimal system for precipitation of zirconium phosphonate **2**. Under these conditions, we found that when 50 mg of zirconium phosphonate **1–4** was used, excellent recoveries of 95–100% could be achieved.

Conclusions

In conclusion, we have prepared for the first time mesoporous layered zirconium phosphonates with complexing groups and good organosolubility. These zirconium phosphonates possess different solubilities in organic solvents, and this can be utilized to recycle them by precipitation. Owing to their layered mesoporous structures, these zirconium phosphonates could act as catalyst supports, enabling one to take advantage of the site isolation effect, the confinement effect and the cooperation effect, and bridging the gap between heterogeneous catalysts and homogeneous catalysts.

Finally, if a *chiral* β -aminoalcohol is used in the organic moieties of **1–4**, these zirconium phosphonates could have potential application in asymmetric transformations, such as aldol, Mannich and Michael reactions, paving the way for the use of solid base in homogeneous asymmetric catalysis.

Acknowledgements

We are grateful to the Chongqing Scientific Foundation, P. R. China (CSTC, 2007BB4368), for the support of this work.

References

- (a) C. E. Song, *Annu. Rep. Prog. Chem., Sect. C: Phys. Chem.*, 2005, **101**, 143; (b) A. Cormaa and H. Garciaa, *Adv. Synth. Catal.*, 2006, **348**, 1391.
- (a) R. S. Drago and D. C. Pribich, *Inorg. Chem.*, 1985, **24**, 1983; (b) C. E. Song, J. S. Lim and S. C. Kim, *Chem. Commun.*, 2000, 2415; (c) M. W. McKittrick and C. W. Jones, *J. Am. Chem. Soc.*, 2004, **126**, 3052; (d) M. W. McKittrick and C. W. Jones, *J. Catal.*, 2004, **227**, 186; (e) M. W. McKittrick and C. W. Jones, *Chem. Mater.*, 2003, **15**, 1132.
- (a) C. Li, *Catal. Rev.*, 2004, **46**, 419; (b) H. Zhang, Y. Zhang and C. Li, *J. Catal.*, 2006, **238**, 369.
- (a) V. Ayala, A. Corma and M. Iglesias, *J. Catal.*, 2004, **224**, 170; (b) B. Pugin, H. Landert, F. Spindler and H. U. Blaser, *Adv. Synth. Catal.*, 2002, **344**, 974; (c) Q. H. Fan, Y. M. Chen and X. M. Chen, *J. Am. Chem. Soc.*, 1999, **121**, 7407; (d) D. Z. Jiang, F. Xi and A. S. C. Chan, *Chem. Commun.*, 2000, 789; (e) S. J. Liu, H. Y. Cheng, F. Y. Zhao, J. Y. Gong and S. H. Yu, *Chem. Eur. J.*, 2008, **14**(13), 4076; (f) J. Wang, J. C. Groen, W. Yue, W. Zhou and M. O. Coppens, *J. Mater. Chem.*, 2008, **18**(4), 468.
- (a) D. E. Bergbreiter, *Chem. Rev.*, 2002, **102**, 3345; (b) S. Bastin, R. J. Eaves and C. W. Edwards, *J. Org. Chem.*, 2004, **69**, 5405; (c) G. J. Deng, B. Yi and Y. Y. Huang, *Adv. Synth. Catal.*, 2004, **346**, 1440; (d) G. E. Oosterom, J. N. H. Reek and P. C. J. Kamer, *Angew. Chem. Int. Ed.*, 2001, **40**, 1828; (e) R. van Heerbeek, P. C. J. Kamer and P. W. N. M. van Leeuwen, *Chem. Rev.*, 2002, **102**, 3717.
- (a) For examples see: A. Hu, H. L. Ngo and W. Lin, *J. Am. Chem. Soc.*, 2003, **125**, 11490; (b) C. V. Kumar and A. Chaudari, *J. Am. Chem. Soc.*, 2000, **122**, 830; (c) U. Costantino, M. Curini and O. Rosati, *Curr. Org. Chem.*, 2004, **8**, 591; (d) X. Wu, X. Ma and Y. Ji, *J. Mol. Catal. A: Chemical*, 2007, **265**(1–2), 316; (e) B. Zheng, X. Wu, X. Ma, L. Xiao, Y. Ji and X. Fu, *Catal. Commun.*, 2007, **8**, 1923; (f) H. L. Ngo, A. Hu and W. Lin, *J. Mol. Catal. A: Chemical*, 2004, **215**, 177.
- For examples see: (a) K. Huang, J. Yu and G. Wang, *Eur. J. Inorg. Chem.*, 2004, **14**, 2956; (b) M. J. de la Mata and O. Juanes, *Angew. Chem. Int. Ed.*, 2004, **43**, 619; (c) J. A. Fry, C. R. Samanam, J. L. Montcharnp and A. F. Richards, *Eur. J. Inorg. Chem.*, 2008, **3**, 463.
- For a review see: D. E. Bergbreiter, *Topics In Current Chemistry*, 2004, **242**, 113.
- R. Dragone, P. Galli, M. A. Massucci and M. Trombetta, *J. Mater. Chem.*, 2003, **13**, 834.
- (a) A. Clearfield and D. G. Smith, *Inorg. Chem.*, 1969, **8**, 431; (b) G. Alberti, U. Costantino, S. Allulli and N. Tomassini, *J. Inorg. Nucl. Chem.*, 1978, **40**, 1113.
- J. C. Amicangelo and W. R. Leenstra, *Inorg. Chem.*, 2005, **44**(6), 2067.
- (a) D. M. Poojary, H. L. Hu, F. L. Campbell and A. Clearfield, *Acta Crystallogr., Sect. B*, 1993, **49**, 996; (b) W. R. Leenstra and J. C. Amicangelo, *Inorg. Chem.*, 1998, **37**, 5317.
- (a) P. L. Gentili, U. Costantino, M. Nocchetti, C. Miliana and G. Favaro, *J. Mater. Chem.*, 2002, **12**, 2872; (b) R. Vivani, G. Alberti, F. Costantino and M. Nocchetti, *Microporous Mesoporous Mater.*, 2008, **107**, 58; (c) A. Clearfield, *Journal of Alloys and Compounds*, 2006, **418**, 128; (d) F. Bellezza, A. Cipiciani, U. Costantino and S. Nicolis, *Langmuir*, 2004, **20**, 5019.
- D. Chakraborty, V. Chandrasekhar and M. Bhattacharjee, *Inorg. Chem.*, 2000, **39**, 23.
- Y. Ji, X. Ma and X. Wu, *Appl. Catal. A: General*, 2007, **332**, 247.